Hydrogen Exchange in a Large 29 kD Protein and Characterization of Molten Globule Aggregation by NMR†

Annika Kjellsson,‡ Ingmar Sethson,§,|| and Bengt-Harald Jonsson*,§

Department of Biochemistry and Department of Organic Chemistry, Umeå University, SE-901 87 Umeå, Sweden, and Molecular Biotechnology/IFM, Linköping University, SE-581 83 Linköping, Sweden

Received July 2, 2002; Revised Manuscript Received October 12, 2002

ABSTRACT: The nature of denatured ensembles of the enzyme human carbonic anhydrase (HCA) has been extensively studied by various methods in the past. The protein constitutes an interesting model for folding studies that does not unfold by a simple two-state transition, instead a molten globule intermediate is highly populated at 1.5 M GuHCl. In this work, NMR and H/D exchange studies have been conducted on one of the isozymes, HCA I. The H/D exchange studies, which were enabled by the previously obtained resonance assignment of HCA I, have been used to identify unfolded forms that are accessible from the native state. In addition, the GuHCl-induced unfolded states of HCA I have also been characterized by NMR at GuHCl concentrations in the 0−5 M range. The most important findings in this work are as follows: (1) Amide protons located in the center of the β-sheet require global unfolding events for efficient H/D exchange. (2) The molten globule and the native state give similar protection against H/D exchange for all of the observable amide protons (i.e., water seems not to efficiently penetrate the interior of the molten globule). (3) At high protein concentrations, the molten globule can form large aggregates, which are not detectable by solution-state NMR methods. (4) The unfolded state (U), present at GuHCl concentrations above 2 M, is composed of an ensemble of conformations having residual structures with different stabilities.

Protein folding and stability have been extensively studied, but primarily in smaller model proteins. These smaller proteins frequently display a simple two-state folding mechanism, which may not be representative of processes in larger, more complex proteins. Experiments on some large proteins have indicated that their native states may be reached via folding intermediates (*1*). A compact denatured or molten globule state has been suggested to represent a universal intermediate in the folding pathway (*2*). Characterization of partly (un)folded protein molecules is therefore required for a complete understanding of protein folding and structure. Partly folded conformations are also thought to be important in many other biological processes, such as protein translocation across membranes and formation of the amyloid fibers associated with several neurodegenerative diseases (*3*).

Various unfolded states of the 29 kD isozyme, human carbonic anhydrase II (HCA II), have been characterized by several investigators using different techniques. For instance, the global unfolding parameters of HCA II have been determined by spectroscopically analyzing the effects of denaturants (*4, 5*). These investigations have shown that HCA II unfolds in two transitions, separated by a stable molten globule intermediate (I), which will be referred to in the following text as the first and second unfolding transitions (N ↔ I ↔ U). In addition, the stability of local structures has been investigated using mutagenesis, which has also been exploited, in combination with chemical labeling, to generate various probes (*5*−*8*). The cited techniques have provided detailed information on important aspects of the folding process, but methods that can provide both detailed and more comprehensive data are desired. NMR studies of unfolded forms of the protein, together with hydrogen/deuterium (H/D) exchange experiments in combination with NMR analysis of the protein in mildly denaturing conditions, can provide such information. So NMR has been our chosen method for studying the native and unfolded forms of carbonic anhydrase. Furthermore, we have previously completed the backbone assignment of the isozyme HCA I (*9*), which has a nearly identical backbone structure to HCA II. Results gathered so far show that it unfolds in a manner similar to HCA II and forms a molten globule intermediate at moderate GuHCl concentrations. These findings, and the wealth of relevant information available (especially the completed resonance assignment), have prompted us to study the native and partly unfolded forms of carbonic anhydrase by hydrogen exchange and NMR analyses and to focus our attention on HCA I.

Protons of backbone amide groups, provided they are solvent-accessible, readily exchange with protons of the solvent. Amide protons that are either buried in the interior of the protein or involved in hydrogen bonds exchange slowly since the protein has to unfold, globally or locally, to allow hydrogen exchange to occur. Hence, hydrogen

† This work was supported by a grant from the Swedish Natural Science Research Council to B.-H.J (K5104-5999).

* To whom correspondence should be addressed. Phone: (+46) 13 288935 or (+46) 70 3974520. Fax: (+46) 13 122587. E-mail: nalle@ifm.liu.se.

‡ Department of Biochemistry, Umeå University.

§ Linköping University.

|| Department of Organic Chemistry, Umeå University.

10.1021/bi026364g CCC: $25.00 © 2003 American Chemical Society
Published on Web 12/19/2002

exchange, as monitored by NMR, gives information about both local and global dynamics (*10*).

The structure of HCA I, which has been determined by X-ray (*11*) analysis, is dominated by a 10-stranded β-structure: an open β-sheet spanning the entire molecule that is located in the major domain of the protein and divides the molecule into two halves. One half contains an extensive hydrophobic cluster, and the other half includes the active site and the N-terminal region. The GuHCl-induced molten globule intermediate is characterized by the loss of enzymatic activity and loss of near-UV CD bands, while far-UV CD spectra show that most of the secondary structure is retained in it. Recent studies on the isozyme HCA II have demonstrated that the formation of a molten globule is accompanied with aggregation (*12*). In the present study we have measured rates of hydrogen/deuterium exchange at backbone amide groups under native and mildly denaturing conditions. The GuHCl-induced equilibrium unfolding of HCA I was also monitored by recording HSQC spectra at concentrations between 0 and 4−5 M GuHCl.

MATERIALS AND METHODS

Theory. Proton exchange of amide protons (H_N) in proteins is generally described by (*13*)

$$\text{H-protein}_{\text{closed}} \underset{k_{\text{cl}}}{\overset{k_{\text{op}}}{\rightleftarrows}} \text{H-protein}_{\text{open}} \xrightarrow{k_{\text{rc}}} \text{D-protein}_{\text{closed}} \quad (1)$$

For a protein that is dissolved in D_2O, the H/D exchange can also be described as in eq 1, where k_{op} and k_{cl} are the rate constants for opening and closing events in the protein, and k_{rc} is the rate constant for the H/D exchange at the amide group. Because of their extreme p*K* values, the exchange of amide protons is catalyzed only by H^+ and OH^-. Plotting the logarithms of the exchange rates as a function of pH gives rise to a V-shaped curve with a minimum between 2 and 3. The position of the minimum of the curve along the pH axis depends on the steric blocking and inductive effects of neighboring side chains. The strength of these effects has been calculated (*14*) in studies of poly-DL-alanine and other polypeptides, and rules have consequently been developed to calculate the sequence-specific inductive effects of neighboring amino acid side chains (*14*, *15*). This has enabled accurate predictions to be made of the exchange rates of amide protons in extended oligopeptides (*15*, *16*) and in solvent-exposed, unstructured regions of native proteins (*15*).

Under conditions favoring the folded state (i.e., $k_{cl} \gg k_{op}$), the observed exchange rate, k_{ex}, is given by

$$k_{\text{ex}} = \frac{k_{\text{op}} k_{\text{rc}}}{k_{\text{cl}} + k_{\text{rc}}} \quad (2)$$

Depending on the ratio of k_{rc} to k_{cl}, the following two limiting conditions may be encountered (*13*):

(i) If $k_{cl} \ll k_{rc}$ (EX1-limit), each opening fluctuation leads to an isotope exchange, and eq 1 simplifies to

$$k_{\text{ex}} = k_{\text{op}} \quad (3)$$

In this case, the exchange is limited by the opening rate, k_{op}. Obviously, H_N exchange measurements under EX1 conditions provide readily interpretable data that can be correlated with a key feature of internal protein motility.

(ii) If $k_{cl} \gg k_{rc}$ (EX2-limit), the intrinsic exchange is the rate-limiting step, and eq 1 reduces to

$$k_{\text{ex}} = (k_{\text{op}}/k_{\text{cl}})k_{\text{rc}} = K_{\text{op}} k_{\text{rc}} \quad (4)$$

Here, $K_{op} = k_{op}/k_{cl}$ is the equilibrium constant for the conformational transition between the folded and the unfolded states. In contrast to measurements of k_{ex} under an EX1 regime, k_{ex} resulting from an EX2 process is not directly related to a kinetic process in the protein. Instead, because of the effects of the intrinsic amide proton exchange rate, it shows a linear dependence on pH. However, provided that reliable values for k_{rc} are available (*17*), such measurements can be used to study the equilibria between folded and unfolded states for individual amide protons.

Using eq 4 it is possible to calculate the free energy for the underlying structural opening reaction, according to

$$\Delta G_{\text{op}} = -RT \ln(k_{\text{ex}}/k_{\text{rc}}) \quad (5)$$

The Gibbs free energy of unfolding is often considered to be linearly related to the denaturant concentration

$$\Delta G_{\text{op}}(\text{den}) = \Delta G_{\text{op}}(0) - m[\text{den}]$$

where the slope (*m*) reflects the amount of new denaturant-binding surface exposed upon protein unfolding (*18*). The slope can be determined from equilibrium unfolding studies, and the Gibbs free energy of unfolding at zero denaturant concentration can be extrapolated from these data. Hence, amide protons that can only exchange via global unfolding events will show the same linear relationship. In contrast, the ΔG_{op} values of amide protons that exchange through local unfolding events, where little or no increase in exposed surface occurs, will be largely unaffected by the denaturant concentration. Amide protons involved in such local unfolding events will generally show a transition from $m \sim 0$ to the slope observed for globally exchanging amide protons with increasing denaturant concentration since the global unfolding pathway for these protons will make an increasing contribution to the observed exchange rate.

In addition, there are H_N values that show exchange patterns that never coincide with the global unfolding transition, indicating the presence of partially unfolded forms. It is also possible to observe ΔG_{op} values that are located above the line corresponding to the global unfolding, indicating that these amide protons may be protected by residual structures in the unfolded state (*19*).

Sample Preparation and Exchange Experiments. Escherichia coli strain BL21(DE3), which harbors the plasmid pHCA I (*20*), was grown at 23 °C. HCA I production was initiated by adding IPTG to a final concentration of 0.5 mM when cell density corresponding to an OD_{660} of 0.5 was attained, and the protein was harvested after allowing the cells to grow for a further 6−12 h. Uniformly ^{15}N-labeled HCA I was produced by allowing the cells to grow in a defined medium consisting of (per liter), 0.5 g of (^{15}N)-NH_4Cl, 0.5 g of NaCl, 6 g of Na_2HPO_4, 3 g of KH_2PO_4, 4 g of glucose, 50 mg of ampicillin, and 0.5 mM $ZnSO_4$.

Selective incorporation of ^{15}N-labeled amino acids was accomplished by growing the bacteria in defined media

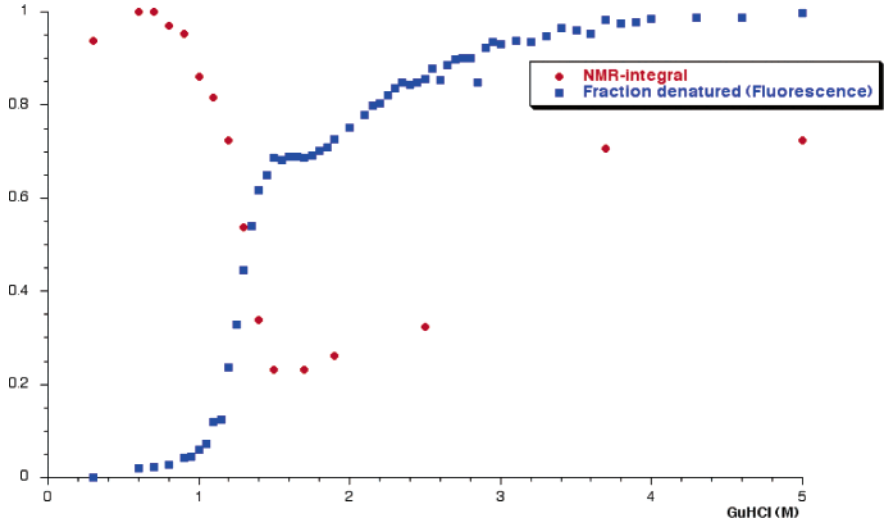

FIGURE 1: Equilibrium unfolding of HCA I, as monitored by fluorescence red-shift and NMR integrals.

containing (per liter): 125 mg of adenine, 125 mg of uracil, 125 mg of cytosine, 125 mg of guanosine, 50 mg of thymine, 50 mg of thiamine, 0.1 mg of biotin, 50 mg of nicotinic acid, 5 g of glucose, 1 g of $^{15}NH_4Cl$, 2 g of sodium acetate, 2 g of succinic acid, 10 g of K_2HPO_4, 500 mg of $MgSO_4$, 5 mg of $FeSO_4$, 400 mg of Ala, 400 mg of Glu, 400 mg of Gln, 400 mg of Arg, 250 mg of Asp, 100 mg of Asn, 50 mg of Cys, 400 mg of Gly, 100 mg of His, 100 mg of Ile, 100 mg of Lys, 250 mg of Met, 100 mg of Pro, 1600 mg of Ser, 100 mg of Tyr, 100 mg of Val, 50 mg of Phe, 100 mg of Leu, 50 mg of Trp, and 100 mg of carbenicillin. In each case, the specific ^{15}N-labeled amino acid(s) used in the experiments was/were added at a 3−5-fold higher concentration than stated above.

The protein was purified to homogeneity in one step with affinity chromatography (*21*), and the purified protein was examined by SDS−PAGE. Protein concentrations were determined from the absorbance of solutions at 280 nm assuming $\epsilon = 49\ mM^{-1}\ cm^{-1}$ (*22*).

Initial attempts to dissolve the protein directly in D_2O gave irregular intensities in the first NMR spectra in the exchange experiments. So, in subsequent experiments the first step in preparing NMR samples for hydrogen exchange experiments was to dissolve 15 mg of lyophilized enzyme in 125 μL of H_2O, resulting in a 4 mM protonated protein solution. The samples were then left to preequilibrate for 12 h as a concentrated protein solution in H_2O, after which H/D exchange was initiated by dilution in sodium phosphate buffer (pH_{read} 7.5) D_2O solutions, containing GuDCl in a range of concentrations (0, 0.3, 0.6, 0.8, 1.0, and 1.2 M), to a final protein concentration of 0.8 mM. ^1H-^{15}N 2-D ge-HSQC-spectra (*23*) of the resulting uniformly labeled protein were obtained following dilution of the protonated enzyme, with an acquisition time of 30 min, at a series of time intervals at 30 °C. A total of 10−20 time points, depending on the exchange rates at the various denaturant concentrations, were obtained for each denaturant concentration. The first 10 spectra were recorded back to back, but subsequent spectra were recorded at increasing time intervals. The experiments were performed on a Bruker DRX-600 spectrometer equipped with a triple-resonance gradient probe.

Determination of Amide Proton Exchange Rates. The peaks for the individual H_N values in the HSQC spectra were integrated by summing all data points constituting the peak. The decaying signals were then fitted to a first-order single-exponential curve of the form $I_t = A_0 + I_0 \exp(-k_{ex}t)$, where I_t is the peak volume at time t, k_{ex} is the first-order rate-constant, and A_0 is the final level determined by the program. The presented exchange rates have a standard deviation of approximately ±14%, corresponding to a standard error in ΔG of ±3%.

Equilibrium Unfolding Studies. The unfolding parameters were determined as described in ref *24*, using fluorescence to monitor the GuHCl-induced unfolding process, except that the temperature was 30 °C, and the pH_{read} was 7.5. The measurements were taken using a Shimadzu RF 5000 spectrofluorometer.

RESULTS

NMR Investigations of the Unfolding of HCA I at Equilibrium Conditions. In this study we investigated the equilibrium between the various folding/unfolding states of HCA I using both NMR and fluorescence measurements. The fluorescence measurements showed that the unfolding of the protein occurs via two or more transitions with an observed intermediate that is the most abundant species between 1.4 and 2 M GuHCl (Figure 1). However, the 2-D ^1H-^{15}N-HSQC NMR spectra recorded in the presence of various concentrations of GuHCl did not display changes reflecting the transitions observed in the fluorescence measurements. Instead, the NMR spectra recorded at GuHCl concentrations below 1.3 M display a nativelike pattern, whereas spectra recorded at GuHCl concentrations above 1.4 M are reminiscent of spectra yielded by unstructured polypeptides (Figure 2). However, more careful inspection of the spectra reveals that those recorded at GuHCl concentrations between 1.0 and 1.4 M, corresponding to the beginning of the N ↔ I transition region, represent superimpositions of native and unfolded spectra, and their relative contributions shifted toward the unfolded form as GuHCl concentrations rose. Simultaneously with these observed spectral changes, the integrated area of all resonances in the 2-D ^1H-^{15}N-HSQC spectra decreased continuously as GuHCl levels increased (Figure 1). The integrated area remains low at GuHCl concentrations between 1.5 and 2.0 M GuHCl, where the

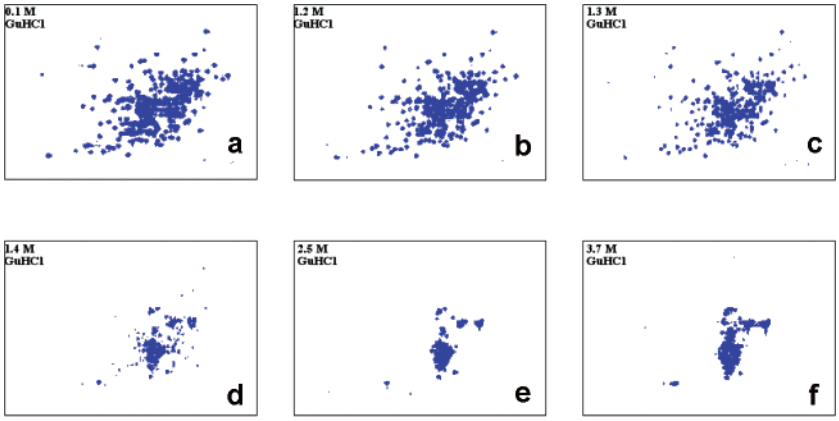

FIGURE 2: 2-D NMR spectra of HCA 1 at various GuHCl concentrations.

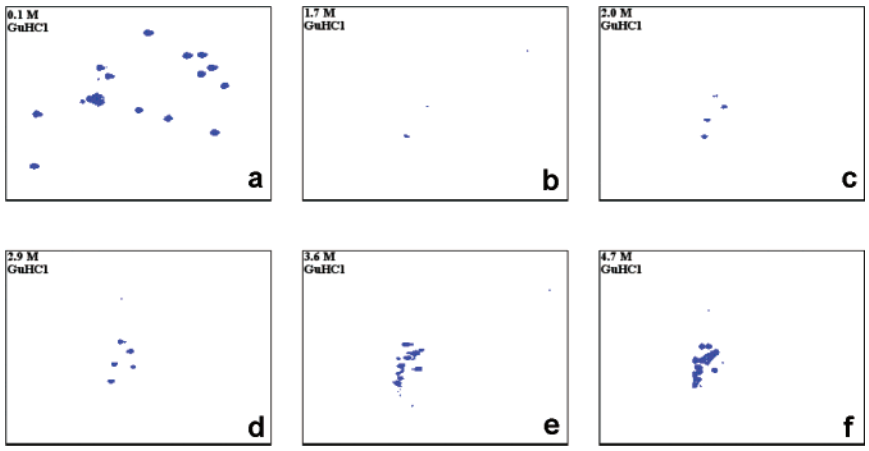

FIGURE 3: 2-D NMR spectra, at GuHCl concentrations ranging from 0.1 to 4.7 M, of ^{15}N-Alanine-labeled HCA I. (a) 0.1 M GuHCl, (b) 1.7 M GuHCl, (c) 2.0 M GuHCl, (d) 2.9 M GuHCl, (e) 3.6 M GuHCl, and (f) 4.7 M GuHCl. The spectral regions displayed in the spectra are those between 7 and 9.3 ppm in the ^{1}H dimension (horizontal axis) and between 113 and 134 ppm in the ^{15}N dimension (vertical axis).

intermediate, according to our interpretation of the fluorescence signals, predominates. The integrated area starts to recover during the I ↔ U transition(s), and there is a gradual increase in the integral thereafter all the way up to 3−4 M GuHCl. The total integral at these high denaturant concentrations is equivalent to only about 70% of the corresponding figure for spectra obtained in the absence of denaturant because of the reduction in the receiver coil quality factor, *Q*, caused by the high concentration of salt. When the effect of salt on the *Q* factor is taken into account, the integrated area at high GuHCl concentrations corresponds to fluoresence from virtually 100% of the protein present. Similar results have previously been reported (*25*).

Inspection of the 2-D spectra of the U state show that clear changes occur in the 2−4 M denaturant concentration range. These observed spectral changes in a uniformly ^{15}N-labeled protein are difficult to interpret because of the significant amount of resonance overlap. To investigate these spectral changes in more detail, 2-D spectra of HCA I labeled with ^{15}N-Alanine, as well as ^{15}N-Alanine/Valine/Phenylalanine/Glycine, were recorded at various GuHCl concentrations (Figures 3 and 4). These spectra show that the intensities of the various resonances increase at different rates when the GuHCl concentration is raised above levels that favor the intermediate. Only one of the 19 Alanine resonances is observable at a denaturant concentration of 1.7 M, and an increasing number of resonances appear in the spectra upon further addition of denaturant (all the way up to 4.7 M), but only four to five resonances are visible between 2 and 3 M denaturant. The NMR spectra of the ^{15}N-AFVG-labeled sample display a quite different pattern (Figure 4). The Glycines (chosen for presentation since they constitute a well-resolved region in the high-field region along the ^{15}N-dimension in the spectra) display four resolved resonances at GuHCl concentrations of just 1.6 M. The remaining Glycine resonances start to reappear in the spectrum at 2.8 M GuHCl, and further changes can be observed all the way up to 3.6 M GuHCl.

H/D Exchange Measured by 2-D ^{1}H-^{15}N NMR. The H/D exchange rates were monitored by recording 2-D ^{1}H-^{15}N-HSQC spectra as functions of time and GuHCl concentration. Since the resolution of the amide proton resonances is restricted in the 2-D NMR spectra of HCA I (*9*), the extended resonance overlap prevented the inclusion of all amino acids in the analysis. The identification of the amide resonances was further complicated by two factors. First, the pH of the HCA I solutions was different in this study as compared to the previous investigation in which the resonance assignments were determined (*9*). Second, the chloride ion concentration varied along with changes in the concentration of the denaturant, GuHCl. Both pH and chloride ion concentration affect the chemical shifts, so the frequencies deviate slightly with respect to the previously published assignment. The pH effect on the shifts was so small that they did not affect the assignments. The maximal Cl^{-} effects on the shifts were generally slightly larger but since each

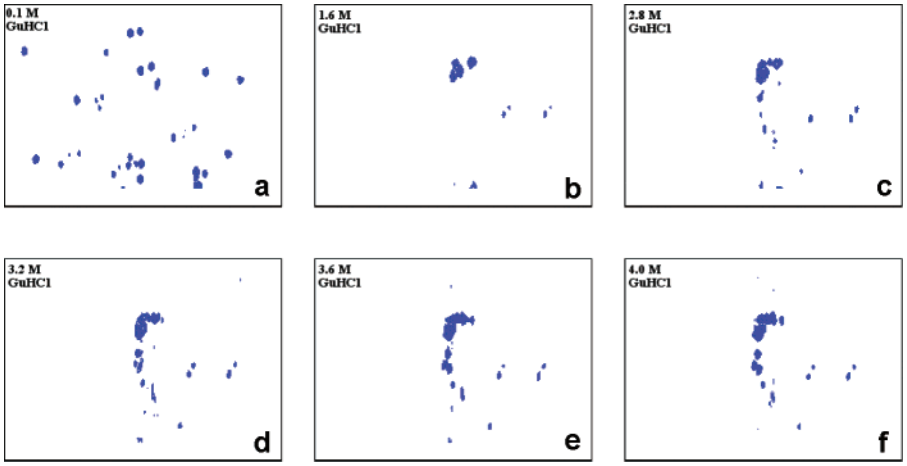

FIGURE 4: 2-D NMR spectra, at GuHCl concentrations ranging from 0.1 to 4.0 M, of ^{15}N-AFVG-labeled HCA I. (a) 0.1 M GuHCl, (b) 1.6 M GuHCl, (c) 2.8 M GuHCl, (d) 3.2 M GuHCl, (e) 3.6 M GuHCl, and (f) 4.0 M GuHCl. The spectral regions displayed in the spectra are those between 6.5 and 10.5 ppm in the ^{1}H dimension (horizontal axis) and between 106 and 119 ppm in the ^{15}N dimension (vertical axis).

resonance shifted by small steps in one direction upon each incremental increase in GuHCl concentration the assignments at the different GuHCl concentrations were obvious. We have chosen to discard all the amide resonances from the analyses if the assignment is ambiguous or if the resonance overlap prevents an accurate integration. With the aid of three sets of specifically ^{15}N-labeled amino acids (Leu, Ile + Ala, and Ala + Phe + Val + Gly), an additional number of very slowly exchanging amide resonances could be identified. This has enabled determination of the exchange behavior of 134 out of the 243 nonproline amino acid residues in HCA I (Figure 5). Sixty-one of these 134 amino acids were deuturated within the dead-time of the experiments, and 45 amino acids exchanged too slowly to allow any quantitative determination of their rate constants. For the remaining 28 amino acids, it was possible to calculate exchange rates, and consequently, ΔG_{op} values at various GuHCl concentrations. The measured exchange rates and calculated ΔG_{op} values are summarized in Table 1. For the more slowly exchanging amide protons (marked in red in Figure 5), it was possible to measure exchange rates at higher GuHCl concentrations (i.e., 0.8−1.2 M). If the exchange at these concentrations was still too slow to allow any exchange rate determination, the minimum possible exchange rates were estimated. The minimum decay rate that would have been statistically significant was chosen when calculating ΔG_{op} values.

H/D Exchange Behavior Related to the Structure of HCA I. The positions in the structure of HCA I of the amino acids with classified exchange behavior are shown in Figures 5 and 6, which give schematic representations of the secondary and 3-D structures of the protein, respectively. As expected, the rapidly exchanging amide protons, marked in blue, are located close to the surface of the protein or in loop regions. However, the amino acids located in the two N-terminal helices also exchange rapidly, which is consistent with earlier observations that these helices do not seem to be well-ordered in solution (*9*). In contrast, the more slowly exchanging amide protons are completely buried, inaccessible to the solvent, and in most cases, also located in the ordered elements of secondary structure.

The amide resonances with intensities that are negligibly affected by H/D exchange (i.e., those marked in red in Figures 5 and 6) all exchange via unfolding events that require at least 10−12 kcal/mol to occur at the lower GuHCl concentrations. These amides are mainly found in the hydrophobic core of the protein. Strands 3−10 in the central β-sheet all contain amide protons that exhibit such slow exchange rates, indicating that a global unfolding event is required to allow their exchange with the solvent (Figure 7). Similar exchange behavior is also observed in the helix located between residues 219−229 for those amide groups in close contact with the central β-sheet (i.e., residues 223, 224, 226, and 227). However, residues 225, 228, and 229, which face the more solvent-exposed side, all exchange via local unfolding events of lower unfolding energies. These observed differences suggest that amide protons in this α-helix that are located closer to the β-sheet are still protected from the solvent when the helix is transiently unfolded. The β-strand located between residues 216−218, which is not a component of the central β-sheet, contains an amide proton that has an equally low exchange rate, as do the residues located in the hydrophobic core of the protein. Notably, this amide proton is in close contact with strand 6 in the central β-sheet (i.e., the most hydrophobic part of the protein). The exchange rate for Leu-185, the C-terminal residue of the short α-helix located between residues 181−185, suggests that global unfolding is necessary for this residue to be accessible to the solvent. Finally, residue 184 in the same helix has exchange rates that are independent of the GuHCl concentration, and its ΔG_{op} value of ∼7 kcal/mol indicates its amide proton is exchanged through a local unfolding event.

DISCUSSION

Previous Studies of the Folding of HCA—A Model for Equilibrium Unfolding. As pointed out in the Introduction, it has been shown, using several techniques, that HCA II unfolds in two well-separated transitions when the GuHCl concentration is raised gradually from 0 to 5 M. Most of the gathered equilibrium unfolding data on HCA II support a three-state model, N ↔ I ↔ U, which includes a compact ensemble of conformations called a molten globule (I). Similarly, the results of this study indicate a molten globule is formed by HCA I, which unfolds in a multistate fashion when the denaturant concentration is raised. The molten globule, which is also characterized by a loss of enzymatic

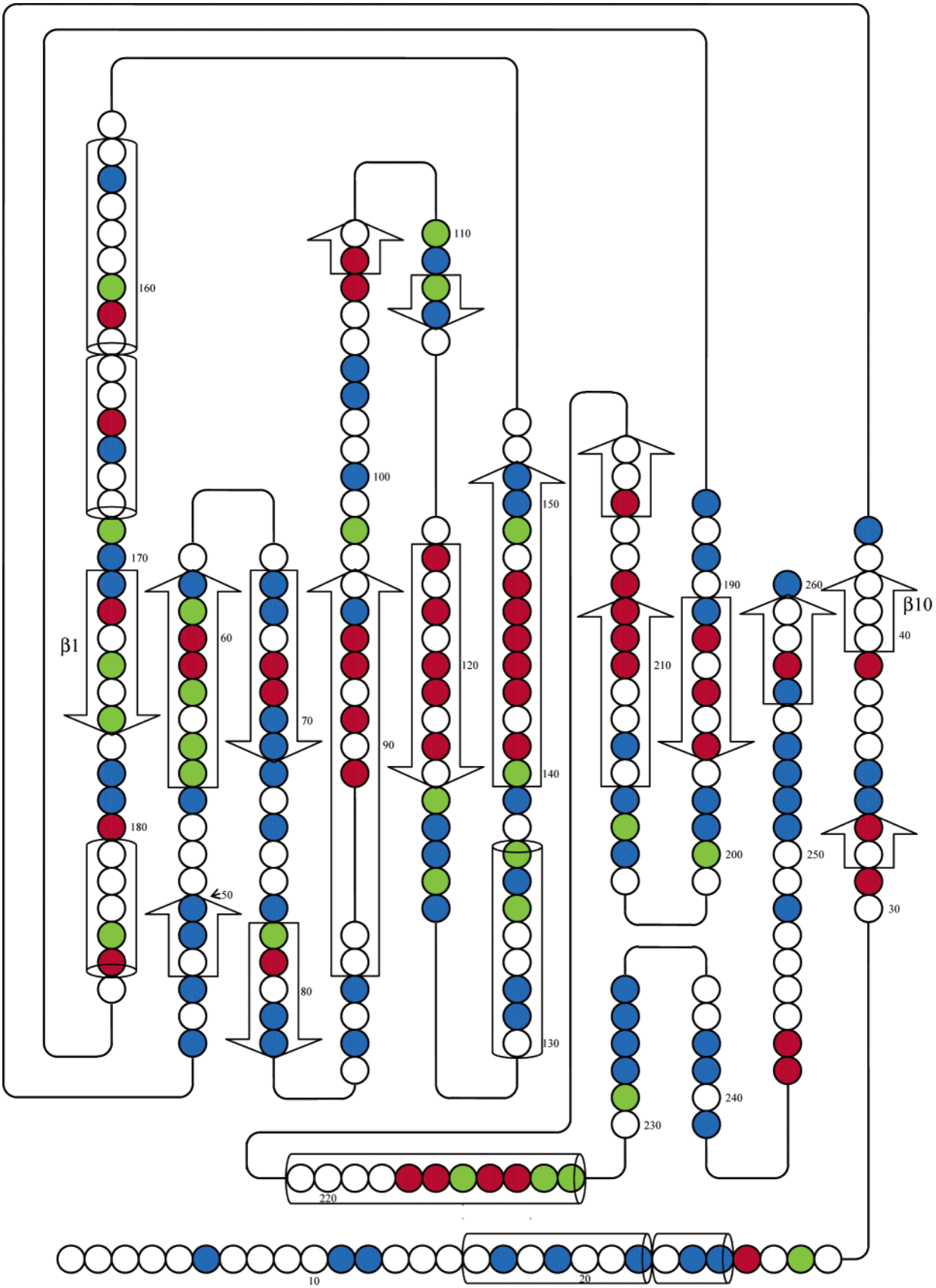

FIGURE 5: Hydrogen exchange pattern and secondary structure. Blue circles represent the residues that have vanished within the dead-time of the experiment; green circles represent the residues where rate constants can be determined at all GuHCl concentrations; red circles represent the residues that do not exchange during the experiments at GuHCl concentrations of 0−0.8 M; and the unfilled circles represent those residues that cannot be evaluated because of residue overlap.

activity, is the most abundant state in a narrower denaturant concentration range for HCA I (1.5−2.0 M) as compared to HCA II (0.8−2.0 M). Earlier studies conducted on HCA II have also shown that the molten globule retains most of the

Table 1: Exchange Rates ($k_{ex} \times 10^3$/s) and Calculated ΔG_{op} values ($\times 10^{-3}$ cal) for the Amino Acids that Have Measurable H/D Exchange Rates

GuHCl (M)	0,0		0.3		0.6		0.8		1.0		1.2		sec. struct.	GuHCl (M)	0,0		0.3		0.6		0.8		1.0		1.2		sec. struct.
a.a.	k_{ex}	ΔG	k_{ex}	ΔG	k_{ex}	ΔG	k_{ex}	ΔG	k_{ex}	ΔG	k_{ex}	ΔG	elem.	a.a.	k_{ex}	ΔG	k_{ex}	ΔG	k_{ex}	ΔG	k_{ex}	ΔG	k_{ex}	ΔG	k_{ex}	ΔG	elem.
N26		*12.4*		*12.4*		*12.4*		*12.4*		*12.4*	0.4	10.2		I144		*10.3*		*10.3*		*10.3*		*10.3*		*10.3*	1.2	7.4	β6
Q28	7.1	8.1	6.2	8.2	6.9	8.1	8.3	8.0	12.9	7.8	16.9	7.6		G145		*11.6*		*11.6*		*11.6*		*11.6*		*11.6*	0.2	9.7	β6
V31		*11.4*		*11.4*		*11.4*	0.02	10.9	1.4	8.4	2.7	8.0		V146		*10.8*		*10.8*		*10.8*		*10.8*		*10.8*	0.5	8.5	β6
I33		*10.3*		*10.3*		*10.3*	0.01	10.2	1.8	7.2	2.0	7.1	β	L147		*10.5*		*10.5*		*10.5*		*10.5*		*10.5*	0.5	8.1	β6
K39		*11.8*		*11.8*		*11.8*		*11.8*	4.6	8.1	1.8	8.6	β10	K149	0.7	9.1	0.4	9.4	1.8	8.5	0.2	9.7	1.7	8.5	0.6	9.2	β6
T55	14.9	7.0	9.9	7.3	8.1	7.4	7.4	7.5	7.5	7.4	6.1	7.6	β2	V160	52.6	5.6	26.9	6.0	20.0	6.2	18.5	6.2	19.2	6.2	14.1	6.4	α4
A56	16.1	7.4	11.1	7.6	11.3	7.6	10.4	7.6	9.8	7.7	8.2	7.8	β2	L161		*10.5*		*10.5*		*10.5*		*10.5*		*10.5*	0.5	8.1	α4
E58	0.3	9.0	0.04	9.7	0.2	8.9	0.02	10.5	1.2	8.2	1.1	8.2	β2	Q165		*11.3*		*11.3*		*11.3*		*11.3*		*11.3*	1.2	8.5	α5
I59		*10.3*		*10.3*		*10.3*		*10.3*		10.3	0.7	7.8	β2	T169	54.1	6.4	47.6	6.5	49.0	6.5	51.6	6.5	108.2	6.2	65.4	6.4	
I60		*9.2*		n.d.		n.d.		n.d.		n.d.		n.d.	β2	K172		*11.7*		*11.7*		*11.7*		*11.7*		*11.7*	1.3	8.8	β1
N61	0.5	9.5	0.3	9.8	1.6	8.9	0.2	10.1	1.3	8.9	2.4	8.6	β2	A174	0.5	9.5	0.2	10.0	1.6	8.8	0.08	10.6	1.2	8.9	1.9	8.7	β1
V68		*10.8*		*10.8*		*10.8*		*10.8*		*10.8*	1.0	7.8	β2	F176	14.0	6.5	10.0	6.7	9.9	6.7	9.2	6.8	9.5	6.7	9.1	6.8	β1
N69		*12.0*		*12.0*		*12.0*		*12.0*		*12.0*	1.8	8.9	β2	D180		*11.2*		*11.2*		*11.2*		*11.2*		*11.2*	0.8	8.5	
V78	2.7	7.6	1.8	7.8	2.3	7.7	1.8	7.9	2.3	7.7	2.4	7.7	β	L184	5.6	7.2	6.9	7.1	7.6	7.0	7.6	7.0	8.4	7.0	7.0	7.1	α6
L79		*10.5*		*10.5*		*10.5*		*10.5*		*10.5*	0.9	7.9	β	L185		*10.4*		*10.4*		*10.4*		*10.4*		*10.4*	0.3	8.5	α6
R89		*11.7*		*11.7*		*11.7*		*11.7*		*11.7*	0.5	9.3	β4	W192		*11.0*		*11.0*		*11.0*		*11.0*		*11.0*	0.5	8.7	β8
F91		*10.9*		*10.9*		*10.9*		*10.9*		*10.9*	0.2	9.3	β4	Y194		*11.4*		*11.4*		*11.4*		*11.4*		*11.4*	0.6	9.0	β8
F93		*11.5*		*11.5*		*11.5*		*11.5*		*11.5*	0.6	9.0	β4	G196		*11.6*		*11.6*		*11.6*		*11.6*		*11.6*	1.2	8.7	β8
H94		*11.5*		*11.5*		*11.5*		*11.5*		*11.5*	0.7	8.9	β4	H200	1.3	8.8	0.4	9.5	2.4	8.4	2.5	8.3	3.6	8.2	2.7	8.3	
G98	0.4	9.6	0.2	10.2	1.1	8.9	0.2	10.0	2.0	8.6	4.2	8.2		Y204	0.5	8.5	1.3	7.9	3.4	7.4	5.4	7.1	18.8	6.3	29.4	6.1	
H107		*11.2*		*11.2*		*11.2*	0.03	10.4	1.9	8.0	3.8	7.6		I210		*10.4*		*10.4*		*10.4*		*10.4*		*10.4*	0.5	8.0	β7
T108		*11.6*		*11.6*		*11.6*	0.04	10.8	1.7	8.5	3.7	8.1	β	I211		*10.2*		*10.2*		*10.2*		*10.2*		*10.2*	0.7	7.7	β7
D110	0.5	8.6	0.4	8.7	0.9	8.2	0.4	8.8	1.8	7.8	3.1	7.5		C212		*12.1*		*12.1*		*12.1*		*12.1*		*12.1*	0.7	9.5	β7
V112	1.0	8.0	1.4	7.8	1.9	7.6	1.5	7.8	2.0	7.6	2.6	7.5	β	K213		*12.2*		*12.2*		*12.2*		*12.2*		*12.2*	0.6	9.7	
A116		*11.0*		n.d.		n.d.		n.d.		n.d.		n.d.	β5	I216		*10.9*		*10.9*		*10.9*		*10.9*		*10.9*	0.4	8.7	β
L118		*10.5*		*10.5*		*10.5*		*10.5*		*10.5*	0.6	8.0	β5	L223		*9.6*		n.d.		n.d.		n.d.		n.d.		n.d.	α7
V120		*10.8*		*10.8*		*10.8*		*10.8*		*10.8*	0.2	9.0	β5	A224		*11.2*		*11.2*		*11.2*		*11.2*		*11.2*	0.3	9.1	α7
A121		*11.3*		*11.3*		*11.3*		*11.3*		*11.3*	0.5	9.0	β5	Q225	2.0	8.4	1.2	8.7	1.2	8.7	0.7	9.1	1.4	8.7	1.0	8.8	α7
W123		*11.2*		*11.2*		*11.2*		*11.2*		*11.2*	0.2	9.2	β5	F226		*11.5*		*11.5*		*11.5*		*11.5*		*11.5*	0.4	9.3	α7
S125	5.7	8.7	3.4	9.0	3.4	9.0	3.3	9.0	4.2	8.9	3.1	9.0		R227		*11.7*		*11.7*		*11.7*		*11.7*		*11.7*	0.5	9.4	α7
Y128	35.8	6.4	18.9	6.8	15.5	6.9	15.9	6.9	14.2	7.0	10.6	7.1		S228	43.5	7.3	22.8	7.7	14.7	8.0	15.5	7.9	19.3	7.8	14.6	8.0	α7
A135	1.3	8.6	0.3	9.5	0.8	8.9	0.1	10.0	1.3	8.6	0.8	8.9	α3	L229	1.1	8.3	0.9	8.4	1.4	8.2	1.1	8.3	1.8	8.0	1.9	8.0	α7
K137	3.5	8.4	3.1	8.4	3.0	8.5	2.7	8.5	3.0	8.5	2.5	8.6	α3	S231	29.7	6.9	28.9	7.0	34.8	6.8	39.7	6.8	68.6	6.5	1.4	9.0	
G140	1.3	8.7	1.4	8.7	1.5	8.6	1.2	8.8	1.6	8.6	1.5	8.6	β6	Q242		*11.8*		*11.8*		*11.8*		*11.8*		*11.8*	0.3	9.8	
L141		*10.0*		n.d.		n.d.		n.d.		n.d.			β6	H243		*11.7*		*11.7*		*11.7*		*11.7*		*11.7*	0.5	9.3	
V143		*10.6*		*10.6*		*10.6*		*10.6*		*10.6*	0.6	8.1	β6	R257		*11.4*		*11.4*		*11.4*		*11.4*	3.3	8.0	5.4	7.7	α9

[a] Minimal ΔG_{op} values are estimated for amino acids that do not exchange in the time range of the measurements. These values are shown in italics; n.d. = not detected.

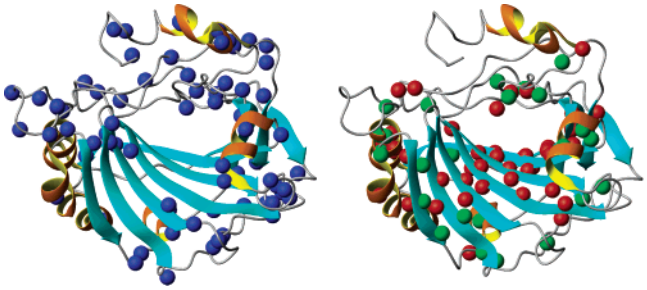

FIGURE 6: Hydrogen exchange pattern and the 3-D structure of HCA I. The symbols are represented as in Figure 5.

native protein's secondary structure, and recent studies have shown that the solvent does not penetrate into the interior of proteins in a molten globule state more efficiently than when they are in their native state (*26*, *27*). Previous investigations of chemical accessibility to amino acid side chains have indicated that only the outer β-strands of the central β-sheet are more exposed in the molten globule than in the native state (*5*, *6*). These studies have also demonstrated that the hydrophobic core region contains structures that are not completely ruptured, even at GuHCl concentrations >5 M.

However, recent investigations (*12*) indicate that equilibrium unfolding is perturbed by protein−protein interactions in the molten globular state leading to the formation of stable protein aggregates (I_{agg}). To accommodate these findings, and the present results, we suggest an extended model for the equilibrium unfolding of HCA:

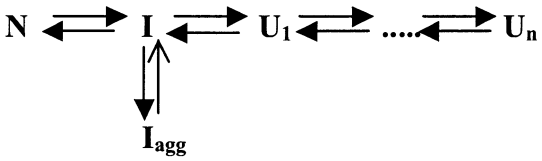

where I_{agg} represents a soluble aggregated state, and U_1 and U_n are ensembles of unfolded states with various degrees of compact or partly structured regions.

The present study can be divided into two parts that are discussed in detail below. In the first part we performed H/D exchange experiments under native and mildly denaturing conditions, which lead to little or no formation of aggregates. The H/D exchange patterns were monitored by NMR and used for detailed characterization of the stability and dynamics of the nonaggregated protein. In the second part, we recorded NMR spectra for samples in which the protein was denatured by GuHCl at concentrations between 0 and 5 M. The results from the second part have given information about properties of the aggregated state (I_{agg}) and the sequential formation of various unfolded states (U).

I. H/D Exchange Studies. The amide protons in HCA I can be divided into three main classes according to their exchange properties:

(i) Rapidly exchanging amide protons that are deuterated prior to the recording of the first NMR spectrum in the exchange experiments.

(ii) Amide protons that are deuterated by local unfolding events, where the exchange rates are largely independent of denaturant concentration.

(iii) Highly protected amide protons that have measurable exchange rates only at GuHCl concentrations of 0.8 M or more, indicating that they are only accessible to solvent molecules following global unfolding events.

The rapidly exchanging amide protons are, as expected, mainly located in loop regions and on the surface of the protein, and thus, carry little information about the folding/unfolding reactions since they are easily accessible to the solvent in the native state.

The exchange rates of the more slowly exchanging amide protons provide information that allows H_N values deuterated by local fluctuations (marked in green in Figures 5 and 6) to be distinguished from those requiring changes in unfolded states for exchange to occur (marked in red in Figures 5 and 6). Unfortunately, the exchange rates of the latter are so slow at denaturant concentrations below 0.8 M that it is not possible to calculate any ΔG_{op} for the corresponding unfolding reaction. Hence, it is not possible to identify the amino acids that exchange only when the protein unfolds completely, which would have provided information about the native and unfolded state at low denaturant concentrations.

It has been shown that HCA II refolds rapidly (within 2 ms) to a collapsed, hydrophobic state following reductions in denaturant concentration, accompanied with a large increase in fluorescence intensity, and the difference in amplitude accounts for 90% of the difference in fluorescence between the native and the unfolded states (*28*). This refolding event, corresponding to the U to I folding reactions, is fast as compared to k_{rc}. Accordingly, if this hydrophobic collapse is sufficient to protect amide protons from exchange with the solvent, the H/D exchange will be mediated via the EX2 mechanism. It is likely that exchange occurs by the EX2 mechanism since the amides that exchange most slowly do not have common exchange rates (Figure 8), as would be expected if they were exchanging via a common global unfolding event under EX1 conditions.

To check for the presence of any irreversible transitions from the native monomeric state of HCA I to an aggregated state, NMR spectra of HCA I at various GuHCl concentrations were recorded months after preparation. There was no detectable change in the integrated area of the amide protons as compared to freshly prepared samples. It was concluded that the aggregate is in equilibrium with the monomeric native state of the protein. This observation is highly relevant to the following sections since the occurrence of such irreversible transitions would have complicated the analysis of the H/D exchange data.

Transient Unfolding of Secondary Structures without Other Structural Rearrangements. The amide protons that have measurable exchange rates at all GuHCl concentrations are almost exclusively located in well-defined secondary structure elements and involved in hydrogen bonds, and their calculated ΔG_{op} values are more or less independent of the denaturant concentration. Thus, the measured free energy of unfolding at lower denaturant concentrations is substantially lower than the level extrapolated from the N ↔ I transition in these cases. However, since the exchange is largely independent of denaturant concentration, they all have higher ΔG_{op} values at high GuHCl concentrations than would be expected if they were affected by the N ↔ I transition. This indicates that the amide protons in these amino acid residues exchange with solvent deuterons because of local unfolding events within secondary structures. Such small structural changes will not expose new surfaces to the solvent, which

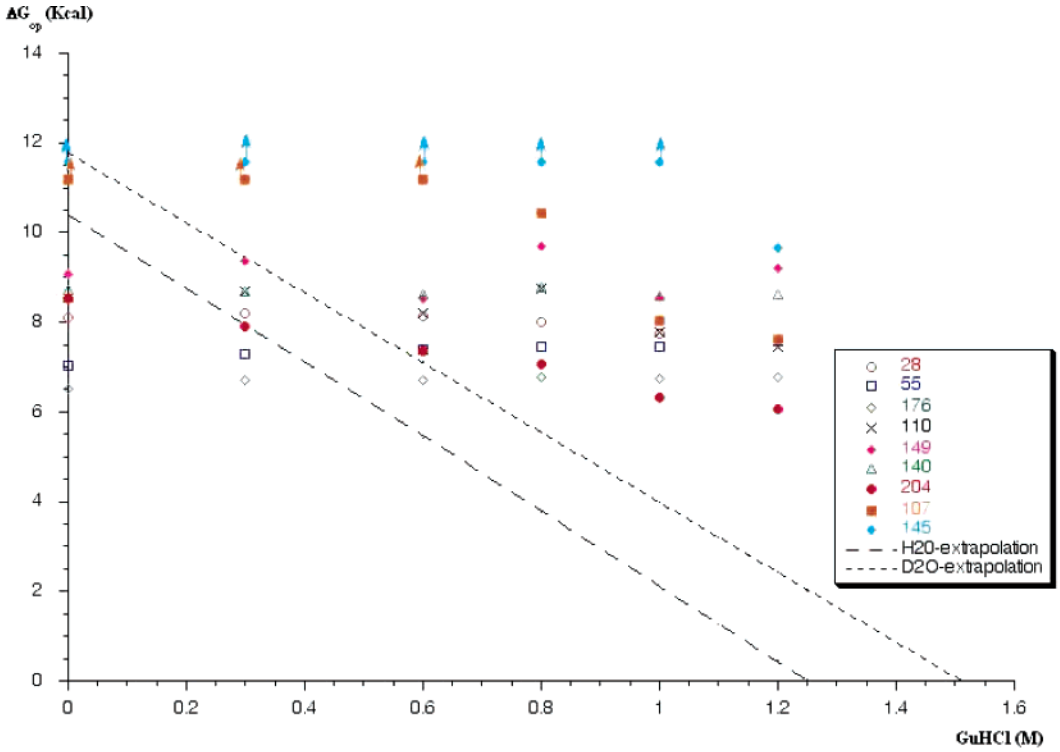

FIGURE 7: ΔG_{op} values as a function of GuHCl concentration for seven of the 28 measurable amino acids and two of the amino acids for which exchange rates could only be calculated at high GuHCl concentrations. The extrapolation from the fluorescence equilibrium measurements (shown in Figure 1) at the first transition is displayed as a broken line. The result from a similar equilibrium experiment performed with D_2O as solvent is shown as a dotted line.

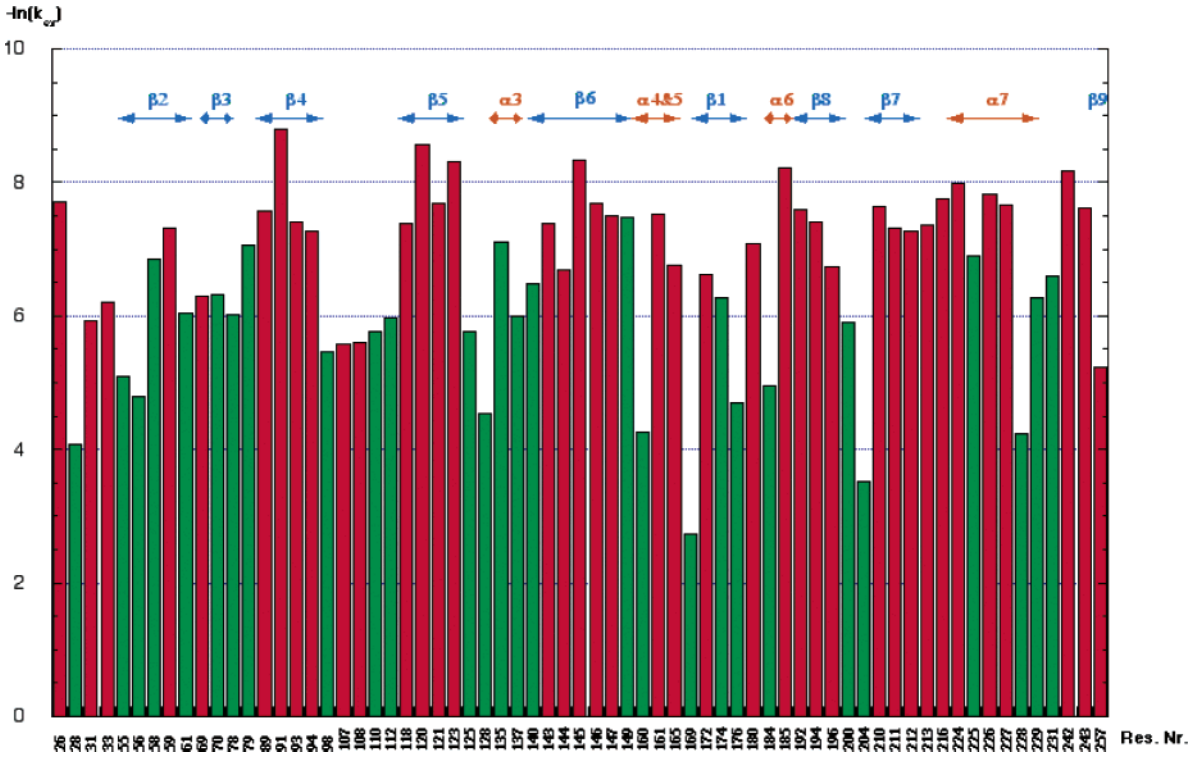

FIGURE 8: Variation in $\ln(k_{ex})$ vs residue number (at 1.2 M GuHCl). The color coding is as in Figure 5 (i.e., red columns represent amino acids that exchange too slowly at GuHCl concentrations below 0.8 M to allow any exchange rate determination, and green columns represent those that could be measured at all GuHCl concentrations).

is why the exchange rates are largely independent of the denaturant concentration. Further support for this interpretation comes from the observation that amide protons within the same secondary structure element can differ in exchange behavior. For instance, in the long helix located under the central β-sheet, the amide protons located on the side of the helix closer to the β-sheet exchange very slowly, whereas those located on the surface-exposed side exchange more rapidly. This can be explained by the assumption that it is not enough to disturb the hydrogen bonds involving the

amide protons close to the β-sheet for exchange to occur. Instead, a larger flip out of the helix, which requires more energy, is needed to mediate H/D exchange for these protons. Similar differences are also observed within several β-strands (e.g., the ends of the strands seem to exchange via local unfolding events), whereas the amino acids closer to the middle require global unfolding. The NMR integrals presented in Figure 1 clearly show that no aggregation occurs at GuHCl concentrations of 0.8 M and lower. Inspection of the H/D exchange results show that all the conclusions that have been drawn so far can be based on results obtained in the GuHCl concentration interval between 0 and 0.8 M. Thus, these conclusions are not affected by the aggregation that is observed to occur at high GuHCl concentrations. Therefore, the H/D exchange results from experiments at 0−0.8 M GuHCl describe fundamental folding properties of the nonaggregated and monomeric protein.

Unfolded State Contains Structured Regions with Different Stabilities. Amide protons that are involved in such slow exchange processes with the solvent that their lifetimes range from months to years are also predominantly found in well-defined secondary structure elements. However, it also seems essential that they are in close contact with the hydrophobic core of the protein to prevent exchange during local unfolding events. Our data suggest that the amide protons of these amino acids are only exchanged following unfolding events that require at least 10 kcal/mol in GuHCl concentrations of 0.8 M or less. The values of ΔG_{op} are high for many of the amide protons observed in experiments between 0 and 0.8 M GuHCl. The highest values are observed for those amide protons that are situated in the part of the β-sheet that is closely associated with the large hydrophobic cluster. It is noteworthy that, to our knowledge, no other protein with this large size has been thoroughly characterized by H/D exchange. Possibly the large hydrophobic cluster can stabilize the associated β-strands more than the corresponding small hydrophobic clusters found in smaller proteins. Thus, we propose that the size of the hydrophobic cluster is correlated to the stability of the associated secondary structures.

For the H/D exchange experiments on protein in 1.0 and 1.2 M GuHCl, it is obvious (from the NMR integration presented in Figure 1) that the results can be affected by the formation of aggregates. Therefore, the remainder of the discussion of exchange data in this section should be seen as suggestions for possible interpretations.

At 1.2 M GuHCl, the ΔG_{op} values determined for these amino acid residues vary between 7 and 10 kcal/mol (Figure 7). If these decaying free energies of unfolding represent a transition to a single unfolded state, one would expect all the residues concerned to converge toward a common ΔG_{op} value at high GuHCl concentrations. Since this is clearly not the case, the variation in the free energy of unfolding implies there are several accessible conformations in U. Alternatively, the observed differences emanate from transient interactions with aggregates. There are in total 16 amino acids that have ΔG_{op} values of 9 kcal/mol or more at 1.2 M GuHCl, implying that they are still protected in the conformations generated by unfolding reactions induced by 7−8 kcal/mol. Of these 16 amino acids, 13 are located in β-strands 4−8 and the helix between residues 219−229. These observations suggest that a residual structure persists in the large hydrophobic core of HCA I at denaturant concentrations higher than 2.5 M. It is notable that these residual structures might be stabilized by interactions with aggregates. Previous studies of HCA II where the chemical accessibility of introduced cysteins was investigated have also indicated the presence of residual structures with different stabilities (*5*). The NMR spectra recorded in the present study (Figures 3 and 4 and section II) also indicate that HCA I adopts a number of different conformations between 2.5 and 5 M denaturant.

N ↔ I Transition Is Not Accompanied by any Detectable Change in Stability of Secondary Structure. The amino acids that contain amide protons with measurable exchange rates (i.e., those marked in green in Figures 5 and 6) all have ΔG_{op} values at low GuHCl concentrations that are significantly lower than the values extrapolated from the N ↔ I transition. Figure 7 shows the free energy for nine representative amino acid residues plotted against the denaturant concentration. Interestingly, none of the amino acid residues show any dependence on GuHCl concentration when crossing the extrapolation from the N ↔ I transition. Hence, none of the identified slowly exchanging amide protons are less protected in the intermediate as compared to the native state, which is consistent with previous observations of the molten globule of HCA II (*26*, *27*) (i.e., the molten globule of HCA I seems to be compact enough to exclude water efficiently from its interior).

II. NMR characterization of HCA I at Equilibrium Conditions at Various GuHCl Concentrations: The Observed Molten Globule Can Form Aggregates. It has previously been observed that HCA II forms soluble aggregates during the refolding process, whereas refolding in the presence of GroEL increases the reactivation yield of the protein (*29*, *30*). These observations indicate that the protein unfolds/refolds via an aggregation-prone state. It has also been demonstrated that the refolding yield is significantly lower when the renaturation is initiated at concentrations of GuHCl favoring the intermediate (*12*). The reactivation yield was found to be mirrored by the two unfolding curves N ↔ I and I ↔ U, respectively, indicating that interactions in the intermediate state occur that promote misfolding upon attempts to refold the protein. The dependence of the width of this refolding trough on the protein concentration suggests that aggregation is likely to be the cause of the low yield of active enzyme upon refolding. In the same study, the diameter of the aggregated equilibrium intermediate was estimated (from dynamic light scattering measurements) to be 13.5 nm in diameter as compared to 4.5 nm for the native protein (*12*). Since no information is available on the shape of the aggregate, the number of protein molecules constituting the aggregate could not be safely estimated. In addition, NMR experiments conducted on HCA II have shown that the intermediate is not detectable by current solution-state NMR methods (Martin Lundqvist, personal communication).

It could be suspected that the failure to observe any NMR signal in the 2-D experiments was due to the delays included in the pulse sequence to achieve the coherence transfer and that the rotational correlation time would be too long to allow detection by solution-state NMR methods. To check this possibility, 1-D proton spectra were also recorded at various GuHCl concentrations. The 1-D spectra revealed the same pattern as the 2-D experiments (i.e., a seemingly sharp transition between the native spectrum and that of a denatured

species, occurring between 1.3 and 1.4 M GuHCl, was also observed when the aliphatic regions of 1-D NMR spectra were inspected). None of the resonances regarded as clear indicators of a native HCA I spectrum (i.e., the α-protons with a chemical shift above 5 ppm and the methyl resonances below 0 ppm) are observable in the spectra recorded at GuHCl concentrations greater than 1.4 M. Since far-UV CD measurements indicate that most of the secondary structure is retained in the intermediate, this provides further evidence that the intermediate is not observable by NMR methods. Furthermore, the integrated area of the aliphatic resonances followed the same trends as the amide protons in the 2-D spectra, confirming that a major fraction of the protein is aggregated and thus cannot be observed by solution-state NMR methods. The inability to observe the intermediate even with 1-D experiments suggests that the aggregate is substantially larger than a tetramer.

I ↔ U Transition Does Not Occur in One Step; the Relative Abundance of Different States Changes with Increasing Denaturant Concentration. There are clear changes in the 2-D spectra of the U state at various denaturant concentrations in the 2−4 M range. From the spectra of proteins labeled at specific amino acid residues, it is apparent that the intensities of the various resonances increase at different rates when the denaturant concentration is raised (Figures 3 and 4). Thus, the GuHCl titration of HCA I reveals that the relatively broad I ↔ U transition observed in the fluorescence measurements (Figure 1) does not represent a single step but rather a number of conformations of varying accessibility. The reappearance of resonances at different denaturant concentrations can be explained by the presence of a range of aggregation states, provided that only restricted regions of the aggregate are immobilized and that only the more mobile parts are detectable in the NMR experiments. This assumption implies that the more structured regions in the aggregate disappear gradually and/or the sizes of the aggregates are reduced when the GuHCl concentration is raised. Another possible explanation for the staggered reappearance of the resonances in the U state as GuHCl concentration is increased is that exchanging conformers may be present, and coalescence restricts the observation of resonances to those located in unstructured, dynamic regions of the protein. Irrespective of which of these explanations is correct, both models imply that there is a gradual disappearance of the structured regions of HCA I in the U state when the GuHCl concentration is raised.

Taken together, these observations suggest that the intermediate unfolding state of HCA I forms an aggregate, as previously observed for HCA II (*12*). This aggregate may provide such a long rotational correlation time, τ_c, that the resulting fast transverse relaxation obstructs its detection by solution state NMR methods. However, unlike HCA II, it is still possible to observe a NMR spectrum of HCA I at GuHCl concentrations in which the intermediate is stable. This can be ascribed to the relatively narrow region of denaturant concentrations favoring the intermediate, in which a proportion of either the unfolded or the native species is always present. Hence, the observed spectrum represents a superimposition of various ratios of the N and U states. A monomeric form of the I state seems to be present in too low concentrations to be detectable. Furthermore, the U state does not represent a unique conformation, but rather an ensemble of conformations, in which the structured regions are gradually ruptured upon successive additions of denaturant.

CONCLUSIONS

In agreement with earlier studies on HCA II (*26*, *27*), the observed H/D exchange rates indicate that the molten globule state is largely protected from solvent penetration. Thus, in a large protein such as HCA I or HCA II, the presence of a well-ordered tertiary structure around the side chains seems to have little or no effect on amide proton exchange rates. Variations in the observed free energies of unfolding suggest that residual hydrophobic interactions may persist in the central β-strands even at high denaturant concentrations. A number of helices and other β-strands participate in local unfolding events. The molten globule intermediate of HCA I can form large aggregates that escape detection by NMR. The unfolded state of HCA I, as detected by CD and fluorescence measurements, does not represent a unique conformation. Instead, the unfolded state, present at GuHCl concentrations above 2 M, is composed of an ensemble of conformations having residual structures with different stabilities, and GuHCl concentrations of 4−5 M are required to reach an unstructured state.

ACKNOWLEDGMENT

We thank Ms. Katarina Wallgren for excellent technical assistance.

REFERENCES

1. Kim, P. S., and Baldwin, R. L. (1990) Intermediates in the Folding Reactions of Small Proteins, *Annu. Rev. Biochem. 59*, 631−660.
2. Ptitsyn, O. B., Pain, R. H., Semisotnov, G. V., Zerovnik, E., and Razgulyaev, O. I. (1990) Evidence For a Molten Globule State As a General Intermediate in Protein Folding, *FEBS Lett. 262*(1), 20−24.
3. Kelly, J. W. (1996) Alternative conformations of amyloidogenic proteins govern their behaviour X, *Curr. Opin. Struct. Biol. 6*, 11−17.
4. Carlsson, U., Henderson, L. E., and Lindskog, S. (1973) Denaturation and Reactivation of Human Carbonic Anhydrases in Guanidine Hydrochloride and Urea, *Biochim. Biophys. Acta 310*, 376−387.
5. Mårtensson, L.-G., and Jonsson, B.-H. (1993) Characterization of folding intermediates of human carbonic anhydrase II: probing substructure by chemical labeling of SH groups introduced by site-directed mutagenesis X, *Biochemistry 32*(1), 224−231.
6. Svensson, M., Jonasson, P., Freskgård, P.-O., Jonsson, B.-H., Lindgren, M., Mårtensson, L.-G., Gentile, M., Borén, K., and Carlsson, U. (1995) Mapping the folding intermediate of human carbonic anhydrase II. Probing substructure by chemical reactivity and spin and fluorescence labeling of engineered cystein residues X, *Biochemistry 34*(27), 8606−8620.
7. Lindgren, M., Svensson, M., Freskgård, P.-O., Carlsson, U., Jonsson B.-H., Mårtensson, L.-G., and Jonasson, P. (1993) Probing local mobility in carbonic anhydrase: EPR of spin-labeled SH groups introduced by site-directed mutagenesis, *J. Chem. Soc., Perkin Trans. 2 11*, 2003−2007.
8. Hammarstrom, P., Kalman, B., Jonsson, B. H., and Carlsson, U. (1997) Pyrene excimer fluorescence as a proximity probe for investigation of residual structure in the unfolded state of human carbonic anhydrase II, *FEBS Lett. 420*(1), 63−68.
9. Sethson, I., Edlund, U., Holak, T. A., Ross, A., and Jonsson, B. H. (1996) Sequential assignment of H-1, C-13 and N-15 resonances of human carbonic anhydrase I by triple-resonance NMR techniques and extensive amino acid-specific N-15-labeling, *J. Biomol. NMR 8*(4), 417−428.

10. Englander, S. W., and Mayne, L. (1992) Protein Folding Studied Using Hydrogen-Exchange Labeling and 2-Dimensional NMR, *Annu. Rev. Biophys. Biomol. Struct. 21*, 243−265.
11. Kannan, K. K., Fridborg, K., Bergstén, P.-C., Liljas, A., Lövgren, S., Petef, M., Strandberg, B., Waara, I., Adler, L., Falkbring, S. O., Göthe, P. O., and Nyman, P. O. (1972) Structure of human carbonic anhydrase B, *J. Mol. Biol. 63*, 601−604.
12. Hammarstrom, P., Persson, M., Freskgard, P.-O., Martensson, L.-G., Andersson, D., Jonsson, B.-H., and Carlsson, U. (1999) Structural Mapping of an Aggregation Nucleation Site in a Molten Globule Intermediate, *J. Biol. Chem. 274*(46), 32897−32903.
13. Hvidt, A., and Nielsen, S. O. (1966) *Adv. Protein Chem. 21*, 287−386.
14. Bai, Y. W., Milne, J. S., Mayne, L., and Englander, S. W. (1993) Primary Structure Effects On Peptide Group Hydrogen-Exchange, *Proteins: Struct., Funct., Genet. 17*(1), 75−86.
15. Molday, R. S., Englander, S. W., and Kallen, R. G. (1972) Primary Structure effects on peptide group hydrogen exchange, *Biochemistry 11*(2), 150−158.
16. Bai, Y. W., Milne, J. S., Mayne, L., and Englander, S. W. (1994) Protein Stability Parameters Measured By Hydrogen-Exchange, *Proteins: Struct., Funct., Genet. 20*(1), 4−14.
17. Roder, H., Wagner, G., and Wüthrich, K. (1985) Individual amide proton exchange rates in thermally unfolded basic pancreatic trypsin inhibitor, *Biochemistry 24*, 7407−7411.
18. Pace, C. N. (1986) Determination and analysis of urea and guanidine hydrocloride denaturation curves, *Methods Enzymol. 131*, 266−280.
19. Bai, Y. W., Sosnick, T. R., Mayne, L., and Englander, S. W. (1995) Protein-Folding Intermediates—Native-State Hydrogen-Exchange, *Science 269*(5221), 192−197.
20. Engstrand, C., Jonsson, B.-H., and Lindskog, S. (1995) Catalytic and inhibitor-binding properties of some active-site mutants of human carbonic anhydrase I, *Eur. J. Biochem. 229*(3), 696−702.
21. Khalifah, R. G., Strader, D. J., Bryant, S. H., and Gibson, S. M. (1977) Carbon-13 nuclear magnetic resonance probe of active-site ionizations in human carbonic anhydrase B, *Biochemistry 16*(10), 2241−2247.
22. Nyman, P.-O., and Lindskog, S. (1964) *Biochim. Biophys. Acta 85*, 141−151.
23. Kay, L. E., Keifer, P., and Saarinen, T. (1992) Pure absorption gradient enhanced heteronuclear single quantum correlation spectroscopy with improved sensitivity, *J. Am. Chem. Soc. 114*, 10663−10665.
24. Mårtensson, L.-G., Jonasson, P., Freskgård, P.-O., Svensson, M., Carlsson, U., and Jonsson, B.-H. (1995) Contribution of individual tryptophan residues to the fluorescence spectrum of native and denatured forms of human carbonic anhydrase II X, *Biochemistry 34*(3), 1011−1021.
25. Plaxco, K. W., Morton, C. J., Grimshaw, S. B., Jones, J. A., Pitkeathly, M., Campbell, I. D., and Dobson, C. M. (1997) The effects of guanidine hydrochloride on the "random coil" conformations and NMR chemical shifts of the peptide series GGXGG, *J. Biomolecul. NMR 10*(3), 221−230.
26. Denisov, V. P., Jonsson, B. H., and Halle, B. (1999) Hydration of denatured and molten globule proteins, *Nat. Struct. Biol. 6*(3), 253−260.
27. Jonasson, P., Kjellsson, A., Sethson, I., and Jonsson, B. H. (1999) Denatured states of human carbonic anhydrase II: an NMR study of hydrogen/deuterium exchange at tryptophan-indole-H-N sites, *FEBS Lett. 445*(2−3), 361−365.
28. Jonasson, P., Aronsson, G., Carlsson, U., and Jonsson, B. H. (1997) Tertiary structure formation at specific tryptophan side chains in the refolding of human carbonic anhydrase II, *Biochemistry 36*(17), 5142−5148.
29. Persson, M., Aronsson, G., Bergenhem, N., Freskgard, P. O., Jonsson, B. H., Surin, B. P., Spangfort, M. D., and Carlsson, U. (1995) Groel/Es-Mediated Refolding of Human Carbonic-Anhydrase-Ii-Role of N-Terminal Helices As Recognition Motifs For Groel, *Biochim. Biophys. Acta: Protein Struct. Mol. Enzymol. 1247*(2), 195−200.
30. Persson, M., Hammarstrom, P., Lindgren, M., Jonsson, B. H., Svensson, M., and Carlsson, U. (1999) EPR mapping of interactions between spin-labeled variants of human carbonic anhydrase II and GroEL: Evidence for increased flexibility of the hydrophobic core by the interaction, *Biochemistry 38*(1), 432−441.

BI026364G